Stability of commercial glucanase and β-glucosidase preparations under hydrolysis conditions

The cost of enzymes makes enzymatic hydrolysis one of the most expensive steps in the production of lignocellulosic ethanol. Diverse studies have used commercial enzyme cocktails assuming that change in total protein concentration during hydrolysis was solely due to adsorption of endo- and exoglucanases onto the substrate. Given the sensitivity of enzymes and proteins to media conditions this assumption was tested by evaluating and modeling the protein concentration of commercial cocktails at hydrolysis conditions. In the absence of solid substrate, the total protein concentration of a mixture of Celluclast 1.5L and Novozyme 188 decreased by as much as 45% at 50°C after 4 days. The individual cocktails as well as a mixture of both were stable at 20°C. At 50°C, the protein concentration of Celluclast 1.5L was relatively constant but Novozyme 188 decreased by as much as 77%. It was hypothesized that Novozyme 188 proteins suffer a structural change at 50°C which leads to protein aggregation and precipitation. Lyophilized β-glucosidase at 50°C exhibited an aggregation rate which was successfully modeled using first order kinetics (R^2=0.97). By incorporating the possible presence of chaperone proteins in Novozyme 188, the protein aggregation observed for this cocktail was successfully modeled (R^2=0.96). To accurately model the increasing protein stability observed at high cocktail loadings, the model was modified to include the presence of additives in the cocktail (R^2=0.98). By combining the measurement of total protein concentration with the proposed Novozyme 188 protein aggregation model, the endo- and exoglucanases concentration in the solid and liquid phases during hydrolysis can be more accurately determined. This methodology can be applied to various systems leading to optimization of enzyme loading by minimizing the excess of endo- and exoglucanases. In addition, the monitoring of endo- and exoglucanases concentrations can be used to build mass balances of enzyme recycling processes and to techno-economically evaluate the viability of enzyme recycling.

1 **Stability of commercial glucanase and β-glucosidase preparations under**
2 **hydrolysis conditions**

3 **Rosales-Calderon[1], Oscar; Trajano[1*], Heather L.; Duff[1], Sheldon J.B.**

4 **[1]Department of Chemical and Biological Engineering, University of British Columbia, 2360**
5 **East Mall, Vancouver, BC, Canada, V6T1Z3.**

6 [*]Corresponding author

7 Email addresses:

8   ORC: ocalderon@chbe.ubc.ca

9   HLT: heather.trajano@ubc.ca

10   DP: posarac@chbe.ubc.ca

11   SJBD: sduff@chbe.ubc.ca

12 **Abstract**

13   **The cost of enzymes makes** enzymatic hydrolysis one of the most expensive steps in the

14   production of lignocellulosic ethanol. Diverse studies have used commercial enzyme

15   cocktails assuming that change in total protein concentration during hydrolysis was solely

16   due to adsorption of endo- and exoglucanases onto the substrate. Given the sensitivity of

17   enzymes and proteins to media conditions this assumption was tested by evaluating and

18   modeling the protein concentration of commercial cocktails at hydrolysis conditions. In the

19   absence of solid substrate, the total protein concentration of a mixture of Celluclast 1.5L

20   and Novozyme 188 decreased by as much as 45% at 50°C after 4 days. The individual

21   cocktails as well as a mixture of both were stable at 20°C. At 50°C, the protein

22   concentration of Celluclast 1.5 was relatively constant but Novozyme 188 decreased by as

23   much as 77%. It was hypothesized that Novozyme 188 proteins suffer a structural change at

24   50°C which leads to protein aggregation and precipitation. Lyophilized β-glucosidase (P-β-

25   glucosidase) at 50°C exhibited an aggregation rate which was successfully modeled using

26   first order kinetics (R^2= 0.97). By incorporating the possible presence of chaperone proteins

27   in Novozyme 188, the protein aggregation observed for this cocktail was successfully

28   modeled (R^2= 0.96). To accurately model the increasing protein stability observed at high

29   cocktail loadings, the model was modified to include the presence of additives in the

30   cocktail (R^2= 0.98). By combining the measurement of total protein concentration with the

31   proposed Novozyme 188 protein aggregation model, the endo- and exoglucanases

32   concentration in the solid and liquid phases during hydrolysis can be more accurately

33   determined. This methodology can be applied to various systems leading to optimization of

34   enzyme loading by minimizing the excess of endo- and exoglucanases. In addition, the

35   monitoring of endo- and exoglucanases concentrations can be used to build mass balances

36   of enzyme recycling processes and to techno-economically evaluate the viability of enzyme

37   recycling.

Introduction

Low cost and readily available lignocellulosic materials, such as wheat straw, switchgrass, or poplar are composed of cellulose and other polysaccharides that can be converted to ethanol. Biological processing of lignocellulose is attractive due to its mild operating conditions, and consists of four processing steps: (1) pretreatment of the raw material to expose the cellulose to enzymes, (2) enzymatic hydrolysis to convert polysaccharides to simple sugars, (3) fermentation of sugars to ethanol and (4) separation of ethanol from the fermentation broth (Bommarius et al., 2008).

Enzymatic hydrolysis is a complex reaction where exo- and endoglucanases or cellulases, most commonly from the fungus *Trichoderma reesei*, adsorb on cellulose to release glucooligomers, cellobiose, and glucose. As cellobiose inhibits cellulases activity, β-glucosidase is added to the hydrolysis to cleave cellobiose to glucose (Lu et al., 2002). However, as lignocellulose also contains non-hydrolysable lignin to which cellulases adsorb irreversibly, some cellulases are lost during hydrolysis (Farinas et al., 2010; Jørgensen et al., 2007; Zhou et al., 2009). These factors necessitate a high enzyme load, which increases hydrolysis costs; indeed one of the key economic factors and thus impediments to lignocellulosic ethanol production and commercialization is the amount and cost of enzyme needed for enzymatic hydrolysis (Lynd et al., 2008; Qi et al., 2011). Consequently, enzymatic hydrolysis has been the target of numerous studies (Jørgensen et al., 2007; Taherzadeh and Karimi, 2007). The hydrolysis is affected by multiple factors such as enzyme loading, reaction time, temperature, substrate composition, and inhibitor concentration. Several studies have attempted to increase the efficiency of the enzyme system or to minimize the amount of enzyme needed for hydrolysis (Arantes and Saddler, 2011; Shen and Agblevor, 2008). The recycling of cellulases bound to the residual substrate as well as enzymes in the reaction

61   suspension is relatively new technology that has been gaining popularity because of its potential

62   to decrease enzyme requirements during ethanol production (Qi et al., 2011).

63   In order to quantify the amount of enzymes that can be recycled, it is necessary to understand the

64   concentration changes of endo- and exoglucanases, and β-glucosidase as well as proteins and

65   compounds contained in the enzyme preparations used in the hydrolysis. Commercial enzyme

66   cocktails from Novozyme: Celluclast 1.5L and Novozyme 188 have been widely used as sources

67   of endo- and exoglucanases, and β-glucosidase, respectively, for enzymatic hydrolysis (Arantes

68   and Saddler, 2011; Hu et al., 2013; Kristensen et al., 2007; Qi et al., 2011; Rodrigues et al., 2012;

69   Shi et al., 2011; Zheng et al., 2009) and enzyme recycling by adsorption research (Lu et al., 2002;

70   Qi et al., 2011; Steele et al., 2005; Tu and Saddler, 2010; Tu et al., 2007a, 2007b). Endo- and

71   exoglucanases present in solution after hydrolysis can be recycled by adsorption onto fresh

72   substrate to start a new round of hydrolysis (Qi et al., 2011). Unfortunately, β-glucosidase cannot

73   be simultaneously recycled by adsorption as it either does not adsorb to the substrate (Tu and

74   Saddler, 2010; Tu et al., 2007a) or adsorbs to a far lesser degree than endo- and exoglucanases

75   (Kumar and Wyman, 2009). Therefore fresh β-glucosidase must be added at the beginning of

76   each round of hydrolysis to avoid build-up of cellobiose and subsequent end-product inhibition of

77   cellulase (Qi et al., 2011). The newest commercial cellulase cocktails, such as Cellic CTec3 from

78   Novozyme (Bagsværd, Denmark) and Accellerase TRIO from DuPont Genencor (CA, USA),

79   contains a blend of endo- and exoglucanases and β-glucosidase. Therefore, the use of Celluclast

80   1.5L and Novozyme 188 as enzymes sources are ideal for the enzyme recycling research, since β-

81   glucosidase from Novozyme 188 can be use to complement recycled cellulases.

82   Many of the enzyme recycling and hydrolysis studies rely upon the assumption of constant

83   protein concentration at hydrolysis conditions; however, this assumption has not been evaluated.

84   Enzyme and protein structures determine solubility and activity and can change with pH,

85   temperature, and/or concentration (Morris et al., 2009). Therefore, the protein concentration in

86   solution depends on system conditions, and must be considered in enzyme adsorption and

87   recycling studies. The objectives of this paper are to evaluate the stability of Celluclast 1.5L and

88   Novozyme 188 protein in solution and to model changes in protein concentration at enzymatic

89   hydrolysis conditions in order to support the subsequent development of a mass balances and

90   economic analysis for enzyme recycling.

Materials & Methods

Enzyme preparations

93   Lyophilized powder cellulases from *Trichoderma reesei* (P-cellulase, Cat. No. C8546, Sigma

94   Aldrich) and β-glucosidase from *Aspergillus niger* (P-β-glucosidase, Cat. No. 9033-06-1, Sigma

95   Aldrich) were used as reference enzymes. Commercial enzyme cocktails from Novozyme were

96   also used: cellulase from *T. reesei*, Celluclast 1.5L (129.3 mg protein/mL, 30.7 CBU/mL, 63.8

97   FPU/mL) and β-glucosidase derived from *A. niger*, Novozyme 188 (102.2 mg protein/mL, 626.4

98   CBU/mL). All enzymes were stored at 2°C until use.

Analysis of enzyme activity and protein concentration

100   Cellulases activity was measured following the NREL filter paper assay (Adney and Baker, 2008)

101   and reported in filter-paper units (FPU) per milliliter of solution. β-glucosidase activity was

102   measured using the method described by Wood and Bhat (1988) and reported in cellobiase units

103   (CBU).

104   Protein concentration was measured by the Bio-Rad protein assay, based on the colorimetric

105   method of Bradford (Bio-Rad Laboratories, 2010). This is a dye-binding assay in which the

106   absorbance shift of the dye Coomassie Brilliant Blue G-250 is proportional to the protein

107   concentration. As the Coomassie blue dye binds to primarily basic and aromatic amino acid

108   residues, especially arginine, it is important to select the correct reference protein to accurately

109   quantify protein (Zhu et al., 2009). Therefore, the potential of P-cellulase, P-β-glucosidase, and

110   the widely used Bovine Serum Albumin (BSA) as calibration standards was studied.

111   Calibration standards with a final volume of 10 mL were prepared with Type II* water (Purelab)

112   for each protein concentration at room temperature. Samples of 0.5 mL were taken and

113   centrifuged (RCF 3.44 g, 10 min). The absorbance spectrum was measured for each sample from

114   200 to 700 nm (UV-1800, Shimadzu). The spectrum curves of the two enzymes were identical

115   with three peaks at 264, 312 and 595 nm. Protein content was measured at 595 nm in the present

116   study as it presented a higher and more defined response than those at 264 and 312 nm, and

117   consequently increased measurement sensitivity.

118   The response of BSA was different from P-cellulase and P-β-glucosidase as shown in Figure .

119   Protein calibration curves. Protein calibration curves (solid lines) for P-cellulase and P-β-

120   glucosidase (); and Bovine Serum Albumin (BSA) ()., due to differences in their amino acid

121   compositions (Zhu et al., 2009). As the use of lyophilized enzymes as a calibration standard

122   increases the accuracy in the protein quantification (Zhu et al., 2009), P-cellulase and P-β-

123   glucosidase were used for this study instead of the widely used BSA.

124   **Pretreatment**

125   Oxygen delignification pretreatment of wheat straw was conducted in a 1 L bench top reactor

126   (PARR 4520). The reactor configuration allowed control of temperature, reaction time, NaOH

127   concentration, and oxygen partial pressure. The reactor was charged at a concentration of 4%

128   (w/w) dry wheat straw and 6-10% NaOH (w/w dry biomass), with a total mass of 500 g. The

129   reactor was sealed and purged with nitrogen in order to remove oxygen. The vessel was heated to

130   the desired temperature and then oxygen was bubbled through the reactor at 1 L/min. A mixing

131   speed of 180 rpm was maintained during the entire process. The reaction was stopped by placing

132   the reactor in ice and bringing it to atmospheric pressure. The pretreated biomass was then

133   filtered and washed using a Buchner funnel and Whatman No. 4 filter paper. The substrates'

134   compositions are shown in Error: Reference source not found.

135   **Protein stability**

136   Protein stability was tested by quantifying protein concentration in solution over the course of 80

137   hours. Acetate buffer (50 mM, pH 4.8) supplemented with 0.02% w/v tetracycline and 0.015%

138   w/v cyclohexamide was placed in shakers (150 rpm) in 250 mL Erlenmeyer flasks at 20 or 50°C

139   for one hour in order to achieve thermal equilibrium before the desired amount of lyophilized

140   enzymes or commercial enzyme preparation was added to a 50 mL final volume. Samples of 0.5

141   mL were withdrawn periodically and then centrifuged (RCF 16,904 g, 10 min). The protein

142   concentration of the supernatant was measured.

143   Novozyme 188 protein stability in the presence of pretreated biomass was tested by quantifying

144   the cocktail's protein concentration in solution over the course of 120 hours. Pretreated wheat

145   straw (substrate S or M) was placed in the same buffer used in the initial tests at 5% wt solids

146   concentration. The mixture was placed in a shaker (150 rpm) in 250 mL Erlenmeyer flasks at

147   50°C before the desired amount of Novozyme 188 was added to a 50 mL final volume. Samples

148   of 0.5 mL were withdrawn periodically and then centrifuged (RCF 16,904 g, 10 min) prior to

149   determining protein content.

150   **Results and Discussion**

151   **Stability of commercial enzyme preparations**

152   The enzyme system commonly used for enzymatic hydrolysis is a mixture of cellulases (endo-

153   and exoglucanases) and β-glucosidases. Endo- and exoglucanases adsorb onto the substrate,

154   primarily cellulose and lignin, while β-glucosidase has been reported to either not adsorb to the

155   substrate (Tu and Saddler, 2010; Tu et al., 2007a), or to have a much lower adsorption on lignin

156 than endo- and exoglucanases (Kumar and Wyman, 2009). Even though Celluclast 1.5L and

157 Novozyme 188 contain multiple proteins, enzymes and other compounds, numerous studies have

158 assumed that any change in the total protein concentration during hydrolysis is due to the

159 adsorption of endo- and exoglucanases on substrate (Arantes and Saddler, 2011; Lu et al., 2002;

160 Qi et al., 2011; Tu et al., 2009, 2007b). By this reasoning, the protein concentration of Celluclast

161 1.5L and Novozyme 188 in the liquid phase should remain constant when substrate is absent. The

162 validity of this assumption was tested by monitoring the protein concentration of Celluclast 1.5L

163 and Novozyme 188, for 78 hours without substrate at 50°C, a common hydrolysis temperature.

164 As shown in Figure . Celluclast 1.5L and Novozyme 188 protein concentration as a function of

165 time at 50 °C. Celluclast 1.5L and Novozyme 188 protein concentration in the same solution at

166 different initial concentrations [6 g/L (2.2 FPU/mL) , 3 g/L (1.1 FPU/mL)   and 1.4 g/L (0.5

167 FPU/mL)] over time at 50°C. Lines are added to assist in visualizing trends. The ratio of 5 CBU

168 per FPU was consistent in all trials., the protein concentration decreased by 30 to 45% dependent

169 on the initial enzyme loading.

170 Farinas et al. (2010) reported the activity of endoglucanases and β-glucosidases from a wild-type

171 strain of *A. niger*. All the enzymes showed a high stability at 37°C, however, the activity of β-

172 glucosidases decreased by approximately 28, 20, and 45% after 48, 72 and 96 h incubation at 50

173 °C, respectively. In the same study, a 40 and 60% loss in activity after 24 and 96 h incubation at

174 50 °C was also reported for endoglucanases, which points to temperature as the responsible

175 variable. In our work, precipitate was observed in the centrifuged samples prior to protein

176 quantification and it appeared that the amount of precipitate increased with hydrolysis time.

177 Given our observations and Farinas's previous work, we hypothesized that high temperatures

178 promote protein aggregation causing the concentration of protein in the liquid phase to decrease.

179 To confirm that aggregation is a consequence of temperature, and not other variables, such as

180 shaking (Wang, 2005), Celluclast 1.5L, Novozyme 188, and a mixture of the two were incubated

181 statically at 20°C and 50°C. The protein concentration was monitored for four days as shown in

182 Figure . Cocktail protein concentration at 20oC (A) and 50°C (B). Celluclast 1.5L and Novozyme

183 188 (), Celluclast 1.5L () and Novozyme 188 () protein concentration as a function of time at 20

184 and 50°C. Lines are added to assist in visualizing trends.. At 20°C the protein concentration

185 remained practically constant for Celluclast 1.5L, Novozyme 188 and the mixture of the two

186 cocktails (Figure . Cocktail protein concentration at 20oC (A) and 50°C (B). Celluclast 1.5L and

187 Novozyme 188 (), Celluclast 1.5L () and Novozyme 188 () protein concentration as a function of

188 time at 20 and 50°C. Lines are added to assist in visualizing trends.). However, at 50°C a 34%

189 drop in the total protein concentration was observed. Celluclast 1.5L suffered an 18% decrease in

190 its concentration at 50°C after 4 days, demonstrating remarkable stability at high temperatures.

191 The loss in Celluclast 1.5L protein concentration is similar to the 14% precipitation reported by

192 Chylenski et al. (2012) for a cellulase preparation from *T. reesei* after 124 h at 50°C . In contrast,

193 the protein concentration of Novozyme 188 decreased by 77% in 4 days at 50°C. This decrease in

194 concentration was accompanied by an increase in the quantity of solid matter on the bottom of

195 the flasks, indicating protein precipitation. It is important to note that the arithmetic sum of the

196 individual Celluclast 1.5L and Novozyme 188 protein concentrations at 50°C (initial

197 concentrations of 1.61 g Celluclast 1.5L/L and 1.06 g Novozyme 188/L) is approximately equal

198 to the total protein concentration in the solution of Celluclast 1.5L and Novozyme 188 at 50ºC

199 (initial concentration of 2.703 g proteins /L) for the period of time monitored. Thus the widely

200 held assumption of constant protein concentration during hydrolysis at 50°C is invalid due to the

201 apparent precipitation of proteins from Novozyme 188, possibly due to aggregation.

202 Dekker et al. (1986) reported that Novozyme 188 lost 17 and 72% of its β-glucosidase activity

203 after 48 and 120 h incubation at 50°C. Chundawat et al. (2011) reported a β-glucosidase protein

204 composition of 7.7% in Novozyme 188, with large amounts of amylases (43.6%) and other

205 proteins (42.1%). Therefore, to evaluate if the loss of β-glucosidase activity reported by Dekker

206 et al. (1986) is caused by β-glucosidase aggregation and precipitation, the stability of P-β-

207 glucosidase from *A. niger* in solution at 50°C was examined.

208 **Stability of β-glucosidases from *A. niger***

209 A representation of the overall pathway generally proposed for the protein aggregation

210 (fibrillation) is presented in Figure . Schematic aggregation of proteins. Idealized representation

211 of a general overall pathway to the formation of aggregates (Morris et al., 2009). (Morris et al.,

212 2009). Protein unfolding can be caused by pH changes, organic solvents, heat, protein

213 concentration, shaking, or the presence of other proteins or chemical compounds (Lehninger et

214 al., 2005). It is hypothesized that native enzyme or protein monomer undergoes a conformational

215 change commonly called denaturation. The protein denaturation can, in some cases, lead to the

216 exposure of "sticky" hydrophobic areas. These areas increase the propensity of the monomer to

217 aggregate or "stick" to each other, causing it to become "active" (Morris et al., 2009). The active

218 monomers or unfolded proteins begin to aggregate forming oligomers that ultimately lead to

219 insoluble fibrils or amorphous aggregates.

220 In his study of the thermal denaturation of almond β-glucosidase using differential scanning

221 calorimetry (DSC), Tanaka (1991) found evidence indicating that β-glucosidase undergoes an

222 irreversible structural transformation from its native conformation to a denatured form between

223 pH 4-8 and 50-90°C. Therefore, given the changes in Novozyme 188 protein concentration in this

224 study at similar temperatures, the β-glucosidases in Novozyme 188 may suffer a similar

225 conformational change leading to aggregation and, subsequently, precipitation. In order to

226 develop a kinetic model of β-glucosidase aggregation, we utilized advances made in the field of

227 heat induced β–lactoglobulin aggregation and precipitation, a phenomenon well-studied by the

228 food industry (Verheul et al., 1998).

229 The proposed protein aggregation reaction consists of two steps: the denaturation and the

230 aggregation steps (Verheul et al., 1998). The denaturation step accounts for β-glucosidase thermal

231 denaturation, which was assumed to be an irreversible reaction (Tanaka, 1991):

$$B \xrightarrow{k_1} D^* \tag{1}$$

233 The native β-glucosidase (B) changes its structure as a result of high temperature, producing a

234 denatured form of the enzyme (D*) that then aggregates in a series of irreversible aggregation

235 reactions. It was assumed that only denatured enzymes participate in the aggregation step. These

236 aggregation reactions can be represented as:

$$D^*_\square + D^*_\square \xrightarrow{k_1} D^*_n$$

$$D^*_\square + D^*_n \xrightarrow{k_n} D^*_{n+1} \tag{2}$$

$$D^*_n + D^*_{n+1} \xrightarrow{k_m} D^*_m$$
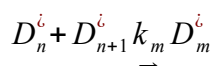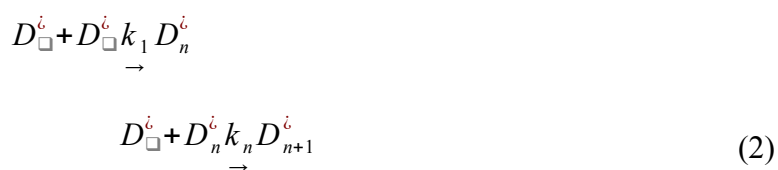
240 $D^*_n, D^*_{n+1},$ and D^*_m are denatured β-glucosidase polymers consisting of n, $n+1$, and m

241 monomeric units (n, $m \geq 2$) and are treated as equivalent species. The aggregation step is

242 comprised of hundreds of autocatalytic reactions (Morris et al., 2009) where denatured polymers

243 adsorb on the aggregate increasing its size and surface area. In consequence, the number of active

244 spots to which denatured polymers can "stick", increases with the growing aggregate. Therefore,

245 the aggregation of each polymer catalyzes the next aggregation reaction and, consequently, the

246 entire aggregation process. In consequence, the aggregates D^*_n, D^*_{n+1} rapidly grow to form the

247 insoluble species D^*_m. According to the Bodenstein principle (Helfferich, 2003), a steady-state

248 situation will be reached quickly once the aggregation reaction starts; the rate at which D* is

249 formed in the denaturation step will equal the rate at which it disappears in the aggregation step

250 (Roefs and De Kruif, 1994). Therefore, the thermal denaturation step (equation 1) is slower than

251 the aggregation step and is thus the rate limiting step. Under this consideration, our analysis

252   assumes only native enzymes to be soluble. From this reaction, assuming first order kinetics, the

253   β-glucosidase rate of disappearance is given by:

254

$$\frac{-d[B]}{dt} = k_1[B] \qquad (3)$$

255   Integrating this equation and taking [B]=[B₀] (g/L) at t=0 gives:

256

$$[¿¿0]e^{-k_1 t} \qquad (4)$$
$$[B] = ¿$$

257   To check the validity of the model, solutions of different P-β-glucosidase concentrations were

258   prepared using powdered P-β-glucosidase and incubated at 50°C. Soluble protein concentration

259   was monitored and, as shown in Figure . Lyophilized β-glucosidase protein concentration

260   changes. Lyophilized β-glucosidase concentration (A) and normalized concentration (B) at 50°C,

261   experimental data ([B0]=0.317 g/L (), 0.612 g/L () and 1.388 g/L ()) and 1st order kinetic model,

262   Equation 4 ()., protein concentration decreased by as much as 84% over 98 h. The protein

263   concentrations shown in Figure . Lyophilized β-glucosidase protein concentration changes.

264   Lyophilized β-glucosidase concentration (A) and normalized concentration (B) at 50°C,

265   experimental data ([B0]=0.317 g/L (), 0.612 g/L () and 1.388 g/L ()) and 1st order kinetic model,

266   Equation 4 (). were used to fit equation 4. The measured initial protein concentrations were used

267   in the model fitting process. The rate constant was determined by least squares regression,

268   obtaining a k_1 of 0.024 h⁻¹. The proposed model had a good fit to the aggregation of P-β-

269   glucosidase experimental data with a R^2= 0.97 as shown in Figure . Lyophilized β-glucosidase

270   protein concentration changes. Lyophilized β-glucosidase concentration (A) and normalized

271   concentration (B) at 50°C, experimental data ([B0]=0.317 g/L (), 0.612 g/L () and 1.388 g/L ())

272   and 1st order kinetic model, Equation 4 ().A. The analysis of the residuals showed that 78% of

273   the predicted P-β-glucosidase concentrations are within one standard deviation of the

274   experimental data. In agreement with the model, the aggregation of P-β-glucosidase does not

275 depend on the initial enzyme concentration as shown in Figure . Lyophilized β-glucosidase

276 protein concentration changes. Lyophilized β-glucosidase concentration (A) and normalized

277 concentration (B) at 50°C, experimental data ([B0]=0.317 g/L (), 0.612 g/L () and 1.388 g/L ())

278 and 1st order kinetic model, Equation 4 ().B.

279 Based on the presented model, 68% of the initial concentration of P-β-glucosidase is lost after 48

280 h incubation at 50°C. However, Dekker et al. (1986) reported an activity loss of 17% for

281 Novozyme 188 and that enzyme activity is linearly related to enzyme concentration. The reported

282 loss in activity is incongruous with the large loss of P-β-glucosidase observed after 48 h

283 incubation; therefore, β-glucosidases in Novozyme 188 seems to be more stable than P-β-

284 glucosidase. As both β-glucosidases come from *A. niger,* the higher apparent stability of β-

285 glucosidases in Novozyme 188 may be caused by the stabilizing effect of the other proteins and

286 compounds in Novozyme 188.

287 **Novozyme 188 stability**

288 Understanding Novozyme 188 protein concentration changes under hydrolysis conditions can

289 provide valuable information about the adsorption-desorption process of endo- and

290 exoglucanases. The interaction of Novozyme 188 with pretreated biomass has to be determine,

291 for this reason, Novozyme 188 protein concentration was monitored in the absence and presence

292 of pretreated wheat straw with 4.7% (substrate S) and 9.0% (substrate M) lignin. Figure . Effect

293 of pretreated biomass on Novozyme 188 protein aggregation. Novozyme 188 protein

294 concentration at 50°C as a function of time in the absence ( ) and presence of pretreated biomass:

295 substrate M () and S (). shows that during the incubation of Novozyme 188 at 50°C the protein

296 concentration profiles in the absence or presence of pretreated biomass were similar and

297 independent of pretreated biomass lignin composition. These results confirm that, independent of

298 lignin concentration, the proteins and enzymes contained in Novozyme 188 do not adsorb to

299 substrate. The results also confirm that the presence of substrate has no impact on the aggregation

300 and precipitation of Novozyme 188 protein.

301 The changes in total protein concentration in solution during enzymatic hydrolysis are most

302 probably caused by Novozyme 188 protein aggregation and adsorption-desorption of exo- and

303 endoglucanases in the substrate. The protein mass balance in solution during hydrolysis is:

$$[¿¿E] = ¿ \atop ¿ \overset{T \atop E}{[¿¿L] + [N]}$$ (5)

304 where the total protein concentration $[T_E]$ (g/L) is defined by the protein concentration of

305 Celluclast 1.5L in solution $[E_L]$ (g/L) and Novozyme 188 protein concentration $[N]$ (g/L) as

306 shown in Figure . Cocktail protein concentration at 20oC (A) and 50°C (B). Celluclast 1.5L and

307 Novozyme 188 (), Celluclast 1.5L () and Novozyme 188 () protein concentration as a function of

308 time at 20 and 50°C. Lines are added to assist in visualizing trends.. Hu et al. (2013) reported that

309 the major cellulase monocomponents within Celluclast 1.5L, on a protein weight basis, were *T.*

310 *reesei* Cel7A, Cel6A, Cel7B, and Cel5A comprising approximately 56%, 12%, 5%, and 6% of

311 the total protein, respectively. However, more cellulases may be present in the cocktail as the *T.*

312 *reesei* genome also includes Cel12, Cel61 and Cel45, as reported by Martinez et al. (2008). From

313 these papers, it can be assumed that Celluclast 1.5L is primarily composed of endo- and

314 exoglucanases. Therefore, the concentration of endo- and exoglucanases in solution $[E_L]$ (g/L),

315 and consequently those adsorbed on substrate, can be indirectly determined by subtracting the

316 Novozyme 188 protein concentration $[N]$ (g/L) from the total protein concentration $[T_E]$ (g/L)

317 measured during hydrolysis. This approximation is possible only if the Novozyme 188 protein

318 concentration can be predicted over the course of the enzymatic hydrolysis.

319 In order to model the aggregation of Novozyme 188, it was assumed that the majority of proteins

320 and enzymes in Novozyme 188 have the same thermal stability. This assumption is supported by

321   the results presented in Figure . Cocktail protein concentration at 20oC (A) and 50°C (B).

322   Celluclast 1.5L and Novozyme 188 (), Celluclast 1.5L () and Novozyme 188 () protein

323   concentration as a function of time at 20 and 50°C. Lines are added to assist in visualizing trends.,

324   where 80% of the initial Novozyme 188 protein concentration is lost after 4 days incubation at

325   50°C showing a consistent response to temperature. As mentioned, some compounds present in

326   Novozyme 188 may stabilize the proteins and enzymes at high temperatures. Due to the reported

327   *A. niger* capacity to produce chaperones (Guillemette et al., 2007; Lu et al., 2010), it was

328   assumed that the proteins and enzymes in Novozyme 188 are stabilized by chaperones.

329   Chaperones are proteins that bind to non-native conformations of proteins and assist them in

330   achieving their native structure. Most chaperones bind to exposed hydrophobic surfaces of non-

331   native species and thereby stabilize the protein or enzyme against aggregation. After being

332   released from the chaperone, the protein may proceed to fold correctly, or rebind to a chaperone

333   until a native conformation is reached (Liberek et al., 2008; Schlieker et al., 2002).

334   The thermal denaturation of protein in Novozyme 188 can be described following the same

335   assumptions and considerations used for the aggregation of P-β-glucosidase. However, a reverse

336   reaction was added to the model to account for the stabilizing effect of chaperones:

337   $$N \underset{k_2}{\overset{k_1'}{\rightleftharpoons}} D^{\dot{\iota}}_{\square} \tag{6}$$

338   where N refers to the native proteins in Novozyme 188 and $D^{\dot{\iota}}_{\square}$ refers to the denatured

339   proteins which interact with chaperones that regenerate their native protein structure. Therefore,

340   the rate of disappearance and formation of native proteins is:

341   $$\frac{-d[N]}{dt} = k_1'[N] - k_2[D^{\dot{\iota}}] \tag{7}$$

342   The amount of protein precipitated is given by $\begin{matrix} D \\ ¿ \\ [¿¿¿]=¿ \\ ¿ \end{matrix}$ N_0]-[N] (g/L), where [N_0] is the initial

343   Novozyme 188 protein concentration (g/L). Solving this equation taking [N]=[N_0] (g/L), at t=0

344   yields:

$$[N]=\frac{[¿¿0]\left(k_2+k'_1 e^{-t\left(k_2+k'_1\right)}\right)}{k_2+k'_1} \qquad (8)$$

345

346   The rate constants in equation 8 were determined by least squares regression to be k'$_1$= 0.017 h^{-1}

347   and k$_2$=0.011 h^{-1}. The measured initial concentrations were used for the model fitting. Equation 8

348   successfully predicts the Novozyme 188 protein concentration in solution at the tested hydrolysis

349   conditions with a correlation coefficient of 0.96, as shown in Figure . Proposed Novozyme188

350   kinetic model incorporating the presence of chaperones. Novozyme 188 concentration (A) and

351   normalized concentration (B) at 50°C: experimental data ([N0]=0.36 g/L (), 0.71 g/L () and 1.44

352   g/L ()) and the chaperone model, Equation 8 ().A. Most of the predicted protein concentrations

353   (75%) are within one standard. Therefore, the proposed model (equation 8) has a good fit to the

354   experimental data in the range of concentrations tested.

355   However, it is clear from Figure . Proposed Novozyme188 kinetic model incorporating the

356   presence of chaperones. Novozyme 188 concentration (A) and normalized concentration (B) at

357   50°C: experimental data ([N0]=0.36 g/L (), 0.71 g/L () and 1.44 g/L ()) and the chaperone model,

358   Equation 8 ().B that the protein aggregation from Novozyme 188 exhibits a peculiar behavior

359   which is not captured by equation 8: the rate of aggregation was slower at higher initial

360   concentrations. These results contradict the aggregation behavior reported for other systems of

361   proteins (Roefs and De Kruif, 1994; Verheul et al., 1998), where the rate of aggregation and

362   precipitation increases with initial concentration (Wang, 2005). Under severe stress conditions,

363 protein aggregation occurs even in the presence of chaperones because the substantial increase in

364 misfolded proteins cannot be buffered by the limited chaperone capacity (Schlieker et al., 2002).

365 Therefore, it is unlikely that the increasing protein stability at increasing Novozyme 188

366 concentrations is caused by the chaperones.

367 Other compounds have been explored for their ability to achieve similar stabilizing effects during

368 denaturation. A common method to stabilize proteins is the use of additives such as sugars,

369 polyols, salts, and surfactants, which have chaperone-like effects. These additives stabilize

370 proteins and suppress aggregation by changing the environmental properties of the proteins

371 (Wang, 2005). Novozyme 188 is a mixture of compounds selected to improve enzyme

372 performance and stability. As Novozyme 188 is a commercial product, its preparation and

373 composition are not public knowledge making it difficult to fully understand its behavior.

374 However, the presence of additives in Novozyme 188 may explain the increasing Novozyme 188

375 stability at high protein concentrations. If additives are present in the cocktail, their concentration

376 increases in proportion to that of Novozyme 188 protein. Therefore, the additives effect in the

377 system becomes stronger as concentration increases.

378 The hypothetical presence of additives was included in the reverse reaction of the proposed

379 model:

$$N \underset{k_2, A_0}{\overset{k_1''}{\underset{\leftarrow}{\rightarrow}}} D_{\square}^{\lower.5ex\hbox{\scriptsize$\iota$}}$$ (9)

381 The denatured proteins ($D_{\square}^{\iota}$) are influenced by the additives (A_o) to regenerate their native

382 structure (*N*). Therefore the rate of disappearance and formation of native protein is now:

$$\frac{-d[N]}{dt} = k_1''[N] - k_2 \overset{A}{\underset{}{\iota}} \overset{[\iota\iota 0][D^{\iota}]}{}$$ (10)

384 The concentration of additives $[A_0]$ (g/L) was assumed constant and proportional to the initial

385 Novozyme 188 protein concentration $[N_0]$ (g/L), as both come from the same solution. The

386 initial additive concentration was assumed to be given by $\left[\frac{A}{N}_0\right]$, where m_c is a

$$\left[\frac{A}{N}_0\right] = m_c$$

387 dimensionless constant. Using these relations, Equation 10 becomes:

388
$$\frac{-d[N]}{dt} = k_1''[N] - k_2 m_c ([N_0] - [N]) \qquad (11)$$

389 Solving this equation using $k_s = k_2 m_c$ and taking $[N]=[N_0]$ (g/L) at t=0 yields:

390
$$[N] = \frac{k_1''\left[\frac{N}{N}_0\right]}{k_1'' + k_s[N_0]} + k_1''\frac{e^{-t(k_1'' + k_s[N_0])}}{k_s[N_0]} \qquad (12)$$

391 The rate constants in Equation 12 were determined by least squares regression to be k_1" = 0.016 h^{-}

392 ^{1} and k_s=0.008 Lg^{-1}h^{-1}. The experimental initial concentrations were used for the model fitting.

393 The value of constant k"$_1$ is similar to the value obtained for k'$_1$ in equation 8, therefore only the

394 reverse reaction is dependent on the presence of additives and thus cocktail loading. Equation 12

395 successfully predicts the concentration of Novozyme 188 in solution with a correlation

396 coefficient of 0.98, as shown in . The residual analysis showed that all the predicted protein

397 concentrations are now within one standard deviation. Based on the residual analysis for

398 equations 8 and 12, it was concluded that the model with the additives consideration (equation

399 12) more accurately represents the protein aggregation observed. This conclusion agrees with the

400 second order Akaike's information criterion (AICc) (Hurvich and Tsai, 2007) calculated for

401 equation 8 (AICc=-5.4) and equation 12 (AICc=-6.1), where the minimum value reflects a better

402 fit to experimental data.

403 The predicted aggregation of Novozyme 188 with the additives model presented in

404 is in better agreement with the experimental results that Novozyme 188 stability increases at

405 high loadings. The model has a good fit to the data at $[N_0]=0.71$ and 1.44 g/L, however, the

406 model poorly predicted the protein aggregation at $[N_0]=0.36$ g/L, as can be seen in . At low

407 cocktail loadings ($[N_0]=0.36$ g/L), the effect of additives is likely minimal. However, the

408 additives concentration, as well as their effect on the system, will increase at higher cocktail

409 loadings ($[N_0]= 1.44$ g/L) thus the additives' stabilizing effect can be seen only at high protein

410 loadings. This behavior is similar to the reduction in aggregation of lysozyme when the

411 concentration of additives such as glycine ethylester, 2-methoxyethanol, KCl, and spermine is

412 increased (Kudou et al., 2003; Shiraki et al., 2005). The similarity of our results with previous

413 additive studies supports our hypothesis that the increasing stability of Novozyme 188 protein

414 concentration at high concentrations is due to the effect of additives.

415 **Conclusions**

416 The successful commercialization of lignocellulosic ethanol rests upon optimization of enzyme

417 cocktails and hydrolysis conditions thus enzyme adsorption to biomass, minimum enzyme

418 loadings and enzyme recycling have been examined in numerous studies. These studies have

419 assumed that the protein concentration at hydrolysis conditions remains constant and that the

420 most significant change in protein concentration during enzymatic hydrolysis is due to adsorption

421 of cellulases on biomass.

422 In this study, this fundamental assumption was tested by employing two widely used commercial

423 enzyme preparations: Celluclast 1.5L and Novozyme 188. The constant protein concentration

424 assumption was found to be invalid when a 46% protein loss from a solution of Celluclast 1.5L

425 and Novozyme 188 was observed after four days incubation at 50°C. Loss of Novozyme 188

426 proteins was determined to be the main cause of this decrease as Celluclast 1.5L protein

427 concentration only slightly decreased (18% after 4 days) at 50°C. The protein loss in Novozyme

428 188 is likely due to heat-induced denaturation which promotes protein aggregation and,

429 ultimately, precipitation.

430 The aggregation of lyophilized β-glucosidase in solution was monitored and successfully

431 modeled by assuming the thermal denaturation reaction was the rate limiting step. However, the

432 high precipitation of lyophilized β-glucosidase observed does not agree with the reported loss of

433 β-glucosidase activity in Novozyme 188. The apparently higher stability of β-glucosidase in the

434 cocktail is believed to be caused by the presence of chaperones in the cocktail. The changes in

435 proteins concentration from Novozyme 188 were modeled considering the presence of

436 chaperones in the cocktail. However, the experimental data exhibited increasing protein stability

437 at high protein loadings, which was not predicted by the model. This behavior was proposed to be

438 caused by additives. The presence of additives was included in the Novozyme 188 aggregation

439 model; this produced a model which successfully describes the decrease in aggregation rate with

440 increasing cocktail loading. The observed Novozyme 188 protein concentration changes are in

441 agreement with previous studies of the aggregation of lysozyme in presence of additives.

442 The thermal instability of Novozyme 188 has not been previously reported and has significant

443 implications for the study of enzymatic hydrolysis. The total protein concentration has been

444 monitored during hydrolysis in past studies to examine the endo- and exoglucanases adsorption-

desorption process. However, given the Novozyme 188 protein aggregation observed in this

work, the adsorption-desorption information obtained may not accurate. Therefore, despite the

enzyme preparation, protein aggregation must be taken in account when measuring protein

concentrations during enzymatic hydrolysis. By combining the measurement of total protein

concentration with the model in this paper, endo- and exoglucanases concentration changes can

be more accurately determined. Endo- and exoglucanases concentration profiles will lead to

greater understanding of the complex adsorption-desorption process during hydrolysis and to

optimize the endo- and exoglucanases loading, consequently, decreasing the ethanol production

cost. Endo- and exoglucanases concentrations profiles during hydrolysis can also help to select

the best time to maximize the amount of recyclable enzymes. The proposed model also enables

mass balances to determine the amount of endo- and exoglucanases that can be recycled and built

a simulation of the ethanol production process with enzyme recycling to evaluate the economics

of such technology for ethanol production.

Acknowledgements

This work was supported by Consejo Nacional de Ciencia y Tecnología (CONACyT) of Mexico,

Agriculture and Agrifood Canada, and NSERC through its Discovery Grant Program. HLT also

thanks the Chemical and Biological Engineering department of the University of British

Columbia for their generous start-up funding.

References

Adney, B., Baker, J., 2008. Measurement of cellulase activities laboratory analytical procedure

   (LAP), Renewable Energy. Colorado.

466 Arantes, V., Saddler, J.N., 2011. Cellulose accessibility limits the effectiveness of minimum

467   cellulase loading on the efficient hydrolysis of pretreated lignocellulosic substrates.

468   *Biotechnology for Biofuels* 3, 1–16.

469 Bio-Rad Laboratories, 2010. Bio-Rad protein assay, Bio-rad. California.

470 Bommarius, A.S., Katona, A., Cheben, S.E., Patel, A.S., Ragauskas, A.J., Knudson, K., Pu, Y.,

471   2008. Cellulase kinetics as a function of cellulose pretreatment. *Metabolic engineering*. 10,

472   370–81.

473 Chundawat, S.P.S., Lipton, M.S., Purvine, S.O., Uppugundla, N., Gao, D., Balan, V., Dale, B.E.,

474   2011. Proteomics-based compositional analysis of complex cellulase-hemicellulase

475   mixtures. *Journal of Proteome Research* 10, 4365–72.

476 Chylenski, P., Felby, C., Østergaard Haven, M., Gama, M., Selig, M.J., 2012. Precipitation of

477   Trichoderma reesei commercial cellulase preparations under standard enzymatic hydrolysis

478   conditions for lignocelluloses. *Biotechnology Letters* 34, 1475–82.

479 Dekker, R.F.H., Assays, E., 1986. Kinetic, inhibition, and stability properties of a commercial p-

480   0-gluwsidase (cellobiase) preparation from Aspergillus niger and its suitability in the

481   hydrolysis of lignocellulose. *Biotechnology and Bioengineering* 28, 1438–1442.

482 Farinas, C.S., Loyo, M.M., Baraldo, A., Tardioli, P.W., Neto, V.B., Couri, S., 2010. Finding stable

483   cellulase and xylanase: evaluation of the synergistic effect of pH and temperature. *New*

484   *Biotechnology* 27, 810–815.

485 Guillemette, T., van Peij, N.N.M.E., Goosen, T., Lanthaler, K., Robson, G.D., van den Hondel, C.

486   a M.J.J., Stam, H., Archer, D.B., 2007. Genomic analysis of the secretion stress response in

487   the enzyme-producing cell factory Aspergillus niger. *BMC Genomics* 8, 158–75.

488 Helfferich, F.G., 2003. Kinetics of homogeneous multistep reactions, 2nd ed. Elseiver *Science*,

489   Amsterdam.

490 Hu, J., Arantes, V., Pribowo, A., Saddler, J.N., 2013. The synergistic action of accessory enzymes

491   enhances the hydrolytic potential of a "cellulase mixture" but is highly substrate specific.

492   *Biotechnology for Biofuels* 6, 112–24.

493 Hurvich, C.M., Tsai, C., 2007. Regression and time series model selection in small samples.

494   *Biometroika* 76, 297–307.

495 Jørgensen, H., Kristensen, J.B., Felby, C., 2007. Enzymatic conversion of lignocellulose into

496   fermentable sugars: challenges and opportunities. *Biofuels Bioprododucts and Biorefining* 1,

497   119–134.

498 Kristensen, J.B., Börjesson, J., Bruun, M.H., Tjerneld, F., Jørgensen, H., 2007. Use of surface

499   active additives in enzymatic hydrolysis of wheat straw lignocellulose. *Enzyme and*

500   *Microbial Technology* 40, 888–895.

501 Kudou, M., Shiraki, K., Fujiwara, S., Imanaka, T., Takagi, M., 2003. Prevention of thermal

502   inactivation and aggregation of lysozyme by polyamines. *European Journal of Biochemistry*

503   270, 4547–4554.

504 Kumar, R., Wyman, C.E., 2009. Access of cellulase to cellulose and lignin for poplar solids

505   produced by leading pretreatment technologies. *Biotechnology Progress* 25, 807–819.

506 Lehninger, A., Nelson, D.L., Cox, M., 2005. *Lehninger principles of biochemistry*, 4th ed. W.H.

507   Freeman & Company.

508 Liberek, K., Lewandowska, A., Zietkiewicz, S., 2008. Chaperones in control of protein

509   disaggregation. *EMBO Journal* 27, 328–35.

510 Lu, X., Sun, J., Nimtz, M., Wissing, J., Zeng, A.-P., Rinas, U., 2010. The intra- and extracellular

511   proteome of Aspergillus niger growing on defined medium with xylose or maltose as carbon

512   substrate. *Microbial Cell Factories* 9, 23–36.

513 Lu, Y., Yang, B., Gregg, D., Saddler, J.N., Mansfield, S.D., 2002. Cellulase adsorption and an

514   evaluation of enzyme recycle during hydrolysis of steam-exploded softwood residues.

515   *Applied Biochemistry and Biotechnology* 98-100, 641–54.

516 Lynd, L.R., Laser, M.S., Bransby, D., Dale, B.E., Davison, B., Hamilton, R., Himmel, M., Keller,

517   M., McMillan, J.D., Sheehan, J., Wyman, C.E., 2008. How biotech can transform biofuels.

518   *Nature Biotechnology* 26, 169–72.

519 Martinez, D., Berka, R.M., Henrissat, B., Saloheimo, M., Arvas, M., Baker, S.E., Chapman, J.,

520   Chertkov, O., Coutinho, P.M., Cullen, D., Danchin, E.G.J., Grigoriev, I. V, Harris, P.,

521   Jackson, M., Kubicek, C.P., Han, C.S., Ho, I., Larrondo, L.F., de Leon, A.L., Magnuson,

522   J.K., Merino, S., Misra, M., Nelson, B., Putnam, N., Robbertse, B., Salamov, A. a, Schmoll,

523   M., Terry, A., Thayer, N., Westerholm-Parvinen, A., Schoch, C.L., Yao, J., Barabote, R.,

524   Barbote, R., Nelson, M.A., Detter, C., Bruce, D., Kuske, C.R., Xie, G., Richardson, P.,

525   Rokhsar, D.S., Lucas, S.M., Rubin, E.M., Dunn-Coleman, N., Ward, M., Brettin, T.S., 2008.

526   Genome sequencing and analysis of the biomass-degrading fungus Trichoderma reesei (syn.

527   Hypocrea jecorina). *Nature Biotechnology* 26, 553–60.

528 Morris, A.M., Watzky, M.A., Finke, R.G., 2009. Protein aggregation kinetics, mechanism, and

529   curve-fitting. *Biochimica et Biophysica Acta* 1794, 375–397.

530 Qi, B., Chen, X., Su, Y., Wan, Y., 2011. Enzyme adsorption and recycling during hydrolysis of

531   wheat straw lignocellulose. *Bioresource Technology* 102, 2881–9.

532 Rodrigues, A.C., Leitão, A.F., Moreira, S., Felby, C., Gama, M., 2012. Recycling of cellulases in

533   lignocellulosic hydrolysates using alkaline elution. *Bioresource Technology* 110, 526–33.

534 Roefs, S.P., De Kruif, K.G., 1994. A model for the denaturation and aggregation of beta-

535   lactoglobulin. *European Journal of Biochemistry* 226, 883–9.

536 Schlieker, C., Bukau, B., Mogk, A., 2002. Prevention and reversion of protein aggregation by

537   molecular chaperones in the E. coli cytosol: implications for their applicability in

538   biotechnology. *Journal of Biotechnology* 96, 13–21.

539 Shen, J., Agblevor, F.A., 2008. Optimization of enzyme loading and hydrolytic time in the

540   hydrolysis of mixtures of cotton gin waste and recycled paper sludge for the maximum

541   profit rate. *Biochemical Engineering Journal* 41, 241–250.

542 Shi, J., Ebrik, M. a, Yang, B., Garlock, R.J., Balan, V., Dale, B.E., Pallapolu, V.R., Lee, Y.Y.,

543   Kim, Y., Mosier, N.S., Ladisch, M.R., Holtzapple, M.T., Falls, M., Sierra-Ramirez, R.,

544   Donohoe, B.S., Vinzant, T.B., Elander, R.T., Hames, B., Thomas, S., Warner, R.E., Wyman,

545   C.E., 2011. Application of cellulase and hemicellulase to pure xylan, pure cellulose, and

546   switchgrass solids from leading pretreatments. *Bioresource Technology* 102, 11080–8.

547 Shiraki, K., Kudou, M., Sakamoto, R., Yanagihara, I., Takagi, M., 2005. Amino acid esters

548   prevent thermal inactivation and aggregation of lysozyme. *Biotechnology progress* 21, 640–

549   3.

550 Steele, B., Raj, S., Nghiem, J., Stowers, M., 2005. Enzyme recovery and recycling following

551   hydrolysis of ammonia fiber explosion – treated corn stover. *Applied Biochemistry and*

552   *Biotechnology* 121, 901–910.

553 Taherzadeh, M.J., Karimi, K., 2007. Enzyme-based hydrolysis processes for ethanol from

554   lignocellulosic materials: a review. *Bioresources* 2, 707–738.

555 Tanaka, A., 1991. Differential scanning calorimetric study of the thermal denaturation of almond

556   beta-glucosidase. *Agricultural and Biological Chemistry* 55, 2773–2776.

557 Tu, M., Chandra, R.P., Saddler, J.N., 2007a. Evaluating the distribution of cellulases and the

558   recycling of free cellulases during the hydrolysis of lignocellulosic substrates.

559   *Biotechnology Progress* 23, 398–406.

560   Tu, M., Chandra, R.P., Saddler, J.N., 2007b. Recycling cellulases during the hydrolysis of steam

561   exploded and ethanol pretreated Lodgepole pine. *Biotechnology Progress* 23, 1130–7.

562   Tu, M., Pan, X., Saddler, J.N., 2009. Adsorption of cellulase on cellulolytic enzyme lignin from

563   lodgepole pine. *Journal of agricultural and food chemistry* 57, 7771–8.

564   Tu, M., Saddler, J.N., 2010. Potential enzyme cost reduction with the addition of surfactant

565   during the hydrolysis of pretreated softwood. *Applied biochemistry and biotechnology* 161,

566   274–87.

567   Verheul, M., Roefs, S.P.F.M., Kruif, K.G. De, 1998. Kinetics of heat-induced aggregation of beta-

568   lactoglobulin. *Agricultural and Biological Chemistry* 8561, 896–903.

569   Wang, W., 2005. Protein aggregation and its inhibition in biopharmaceutics. *International journal*

570   *of pharmaceutics* 289, 1–30.

571   Wood, T.M., Bhat, K.M., 1988. Methods for measuring cellulase activities. *Methods in*

572   *Enzymology* 160, 87–112.

573   Zheng, Y., Pan, Z., Zhang, R., Jenkins, B.M., 2009. Kinetic modeling for enzymatic hydrolysis of

574   pretreated creeping wild ryegrass. *Biotechnology and Bioengineering* 102, 1558–69.

575   Zhou, Y., Su, S., Song, M., Nie, H.-L., Zhu, L.-M., 2009. Improving the stability of cellulase by

576   immobilization on chitosan-coated magnetic nanoparticles modified with α-ketoglutaric

577   acid. *Bioinformatics and Biomedical Engineering* 1–4.

578   Zhu, Z., Sathitsuksanoh, N., Zhang, P., 2009. Direct quantitative determination of adsorbed

579   cellulase on lignocellulosic biomass with its application to study cellulase desorption for

580   potential recycling. *Analyst* 134, 2267–72.

Figures

Figure . Protein calibration curves. Protein calibration curves (solid lines) for P-cellulase and P-β-glucosidase (); and Bovine Serum Albumin (BSA) ().

Figure . Celluclast 1.5L and Novozyme 188 protein concentration as a function of time at 50 °C. Celluclast 1.5L and Novozyme 188 protein concentration in the same solution at different initial concentrations [6 g/L (2.2 FPU/mL) , 3 g/L (1.1 FPU/mL)   and 1.4 g/L (0.5 FPU/mL)] over time at 50°C. Lines are added to assist in visualizing trends. The ratio of 5 CBU per FPU was consistent in all trials.

Figure . Cocktail protein concentration at 20ºC (A) and 50°C (B). Celluclast 1.5L and Novozyme 188 (), Celluclast 1.5L () and Novozyme 188 () protein concentration as a function of time at 20 and 50°C. Lines are added to assist in visualizing trends.

Figure . Schematic aggregation of proteins. Idealized representation of a general overall pathway to the formation of aggregates (Morris et al., 2009).

Figure . Lyophilized β-glucosidase protein concentration changes. Lyophilized β-glucosidase concentration (A) and normalized concentration (B) at 50°C, experimental data ($[B_0]$=0.317 g/L (), 0.612 g/L () and 1.388 g/L ()) and 1st order kinetic model, Equation 4 ().

Figure . Effect of pretreated biomass on Novozyme 188 protein aggregation. Novozyme 188 protein concentration at 50°C as a function of time in the absence ( ) and presence of pretreated biomass: substrate M () and S (). Line is added to assist in visualizing trend.

Figure . Proposed Novozyme188 kinetic model incorporating the presence of chaperones. Novozyme 188 concentration (A) and normalized concentration (B) at 50°C: experimental data ($[N_0]$=0.36 g/L (), 0.71 g/L () and 1.44 g/L ()) and the chaperone model, Equation 8 ().

603 **Figure . Proposed Novozyme188 kinetic model incorporating the presence of additives.**

604 Normalized Novozyme 188 concentration at 50°C: experimental data ($[N_0]$=0.36 g/L (), 0.71 g/L

605 () and 1.44 g/L ()) and the additives model, Equation 12 ().